Refiei, Alireza; Loni, Reyhaneh; Najafi, G.; Sahin, A.Z.; Bellos, Evangelos

Article

Effect of use of MWCNT/oil nanofluid on the performance of solar organic Rankine cycle

Energy Reports

Provided in Cooperation with:
Elsevier

Suggested Citation: Refiei, Alireza; Loni, Reyhaneh; Najafi, G.; Sahin, A.Z.; Bellos, Evangelos (2020) : Effect of use of MWCNT/oil nanofluid on the performance of solar organic Rankine cycle, Energy Reports, ISSN 2352-4847, Elsevier, Amsterdam, Vol. 6, pp. 782-794, https://doi.org/10.1016/j.egyr.2020.03.035

This Version is available at:
https://hdl.handle.net/10419/244076

Energy Reports 6 (2020) 782–794

Contents lists available at ScienceDirect

Energy Reports

journal homepage: www.elsevier.com/locate/egyr

Research paper

Effect of use of MWCNT/oil nanofluid on the performance of solar organic Rankine cycle

Alireza Refiei [a], Reyhaneh Loni [b], G. Najafi [b,*], A.Z. Sahin [c,d,**], Evangelos Bellos [e]

[a] Process Design Development Research Group, Center for Process Systems Engineering, Institute of Autonomous Systems, Universiti Teknologi PETRONAS, Seri Iskandar, Perak, Malaysia
[b] Department of Biosystem Engineering, Tarbiat Modares University, Tehran, Iran
[c] Mechanical Engineering Department, King Fahd University of Petroleum & Minerals, Dhahran, Saudi Arabia
[d] King Abdullah City for Atomic and Renewable Energy (K.A.CARE) Energy Research & Innovation Center, Dhahran, Saudi Arabia
[e] School of Mechanical Engineering, National Technical University of Athens, Greece

ARTICLE INFO

Article history:
Received 13 December 2019
Received in revised form 24 March 2020
Accepted 30 March 2020
Available online xxxx

Keywords:
Solar ORC system
MWCNT/oil nanofluid
Cavity receivers
Economic analyses
Environmental analyses

ABSTRACT

In the current study, a solar-driven organic Rankine cycle (ORC) system was thermodynamically, economically and environmentally investigated. A focal point concentrator with two different cavity-shape receivers was investigated as the ORC heat source. More specifically, the cylindrical and the hemispherical cavity receivers were examined and compared as the most usual and promising choices. MWCNT/oil nanofluid and R113 were used as the solar heat transfer fluid and ORC working fluid respectively. The main aim of this research is an investigation of different cavities in the solar dish and the investigation of the impact of the use of nanofluids in the solar system by different points of view. The results of this work showed that the hemispherical cavity receiver with nanofluid is the most efficient choice with 21.4% system efficiency, while the use of pure thermal oil in the hemispherical cavity leads to 18.9%. On the other hand, the use of the cylindrical cavity leads to 17.8% and 15.8% system efficiency with nanofluid and pure thermal oil respectively. The levelized cost of electricity (LCOE) was 0.077 €/kWh and 0.076 €/kWh for the cylindrical and hemispherical cavity receiver respectively. Moreover, it was concluded that the solar ORC system with the hemispherical cavity receiver as the ORC heat source had resulted in more positive environmental influence related to the cylindrical one.

1. Introduction

Nowadays, renewable energy becomes increasingly important because fossil fuels are depleted and increasing environmental problems such as CO_2 emission, and global warming (Wong and Bachelier, 2014). Investigations and research related to renewable energy have increased (El-Emam and Dincer, 2017). Solar energy is seen as a promising source of renewable energy to supply energy demand. Solar collectors work as heat exchangers that convert the absorbed solar radiation to thermal energy. There are generally two types of solar collectors, including non-concentrating solar collectors and concentrating solar collectors (Qin et al., 2017). Focal Point Concentrator is a type of focal point concentrator in which all incoming solar radiation is concentrated at the focal point, where the absorber is located (Malali et al., 2017). There are two absorber types, one external receiver and one cavity receiver, for the focal point concentrator. The cavity receivers are more efficient than external receivers due to their specific structure.

Some researchers investigated numerically and experimentally the solar dish concentrator with the cavity receiver (Hussain et al., 2017). The solar dish concentrator has been used as an ORC heat source to generate electricity. In another paper, Loni et al. (2016) considered numerically as an ORC heat source a solar dish concentrator with a rectangular cavity receiver. The solar ORC system's structural and operational optimization parameters were presented. They found improved system performance by reducing the diameter of the cavity, reducing inlet temperature and increasing work fluid flow rate. Pavlovic et al. (2017) considered the solar dish concentrator based on exergy analysis with a spiral cavity receptor. Two types of tubes, namely smooth and corrugated tubes have been used as the cavity tube receiver. The solar dish concentrator with the corrugated tube led to the highest performance. In a different study, Pavlovic et al. (2018) compared the efficiency of a dish concentrator with two cavity

* Corresponding author.
** Corresponding author at: Mechanical Engineering Department, King Fahd University of Petroleum & Minerals, Dhahran, Saudi Arabia.
E-mail addresses: g.najafi@modares.ac.ir (G. Najafi), azsahin@kfupm.edu.sa (A.Z. Sahin).

https://doi.org/10.1016/j.egyr.2020.03.035

Nomenclature

$A_{ap,dish}$	Dish aperture area, m^2
h^*	Enthalpy, kJ/kg
I_{beam}	Solar irradiance, W/m^2
$\dot{m}$	Mass flow rate, kg/s
$\dot{Q}$	Rate of heat, W
$\dot{Q}_{evp}$	Rate of available solar heat at the evaporator, W
T	Temperature, K
$\dot{W}$	Power, W

Greek symbols

η	Efficiency

Subscripts

c	Condenser
evp	Evaporator
H	Heat source
L	Cool source
net	Net
ORC	Organic Rankine Cycle
P	Pump
T	Turbine
II	Second law thermodynamic

receiver types like spiral and conical cavities. Using the conical cavity receiver, they find improved solar system efficiency.

Also, during some experimental tests, Loni et al. (2018e,c) and Loni et al. (2018f) examined the application of various nanofluids, such as alumina/oil, silica/oil, and carbon nanotube/oil nanofluids as working fluid of various cavity receiver forms such as hemispheric, cylindrical and cubic. They found increased solar dish concentrator thermal performance using nanofluids compared to oil as the base fluid. In another work, researchers presented a review paper on the implementation of the Nanofluid as the cavity receiver's solar working fluid. They reported the dish concentrator's highest thermal performance with a hemispheric cavity receiver and the application of carbon nanotube/oil nanofluid as the solar working fluid. The application of nanofluids as the solar fluid has been studied by several researchers (Allouhi et al., 2018; Subramani et al., 2018). Khakrah et al. (2018) energetically and exegetically considered a PTC system using alumina/oil nanofluid as the solar working fluid. The influence of different parameters including volume fraction, wind speed and inlet temperature of the nanofluid on energy and exergy performance of the system was studied. They found that the solar system's energy and exergy efficiency decreased and increased, respectively, with the nanofluid's increased inlet temperature. Loni et al. (2018d) energetically and exegetically investigated the solar dish concentrator performance with the use of Al_2O_3/oil and SiO_2/oil nanofluid as the solar working fluid. They presented some experimental relations for predicting the performance of the solar system. In a different research, Loni et al. (2018b) evaluated dish concentrator performance with different oil-based nanofluid. Sadeghi et al. (2019) conducted numerical and experimental studies of solar system performance using Cu_2O/water nanofluid based on energy and energy analysis. Evacuated tube solar collectors with a parabolic concentrator were used as the solar collector. The effect of nanofluid concentration was evaluated. Suggested solar system performance improved by nanofluid application, with higher nanoparticle volume fraction.

Some other researches have been done related to the properties of different nanofluids (Alarifi et al., 2019b; Asadi et al., 2019a, 2020; Duangthongsuk and Wongwises, 2010). Asadi et al. (2019b) experimentally investigated the stability and thermal conductivity of MWCNT-water nanofluid. The main objective of their study determined an optimum ultrasonication time for having the best properties of the nanofluid. They reported that 60 min ultrasonication as the optimum time resulted in the best stability and highest thermal conductivity. Alarifi et al. (2019a) experimentally tested the rheological properties of MWCNT-TiO_2/oil hybrid nanofluid under different conditions such as shear rate, temperature, and concentration rate. They reported that Newtonian behavior had been shown by the nanofluid in all the investigated parameters. Asadi et al. (2019c) presented a review paper related to sonication parameters on nanofluid properties. Different nanofluid parameters were considered including stability, thermophysical properties, and heat transfer of nanofluids. They found thermal conductivity, and viscosity of the nanofluid increased and decreased with sonication time, respectively. Asadi and Pourfattah (2019) experimentally investigated the heat transfer performance of two types of nanofluids including ZnO- and MgO-engine oil nanofluids. They considered viscosity and thermal conductivity of nanofluids under different temperatures and nanofluid concentrations. They reported that MgO-oil nanofluid resulted in better thermal conductivity compared to ZnO-oil nanofluids in the same condition. In another study, Asadi (2018) presented a study related to the selection of effective nanofluid as a heat transfer fluid in different applications. MWCNT-ZnO/oil nanofluid was investigated at different concentrations and different temperatures. He found that maximum thermal conductivity enhancement was 40%. Some researchers (Asadi et al., 2018) experimentally and numerically considered the influence of using hybrid nanofluids as coolant fluid on the performance of a system. They reported increasing thermal conductivity by a maximum 65% using MgO–MWCNT/oil nanofluid.

On the other hand, ORC systems are implemented as effective power generation technology (Fergani et al., 2019; Srinivas and Reddy, 2014; Sarkar, 2018). Various energy sources, such as geothermal, wind, waste heat, etc., can be used as the ORC heat source (Bellos and Tzivanidis, 2018b). Some researchers studied the application of solar absorbed heat as heat supply to ORC systems. Thermodynamic assessment of the solar dish concentrator with a cavity receiver was considered to provide heat to the ORC device (Loni et al., 2016c). Shahverdi et al. (2019) considered a hybrid system including a solar ORC system and a screw turbine to generate power. They used a PTC system as heat supply to the ORC system and waste hydraulic power was used for power generation by the turbine. They found increasing power generation using the suggested coupled screw turbine with the ORC system. Some researchers investigated a solar ORC system with a dish concentrator with a cubical cavity receiver using thermal oil (Loni et al., 2017b). Loni et al. (2019) studied the influence of nanoparticle size and concentration of alumina/oil nanofluid as heat transfer fluid of a focal point concentrator with cavity receiver. The solar system was used to supply heat to the ORC system. They suggested the optimum conditions for the highest performance achievement.

Based on the abovementioned literature review, no research has been conducted on the thermodynamic analysis of a solar ORC system with various shapes of cavity receiver and MWCNT/oil nanofluid application. In the present study, a focal point concentrator with two cavity shapes including cylindrical, and hemispherical cavity receiver, was investigated as the ORC heat source. MWCNT/oil nanofluid and R113 were used as the solar heat transfer fluid, and ORC working fluid, respectively. It should be stated that the experimental data reported by the authors in

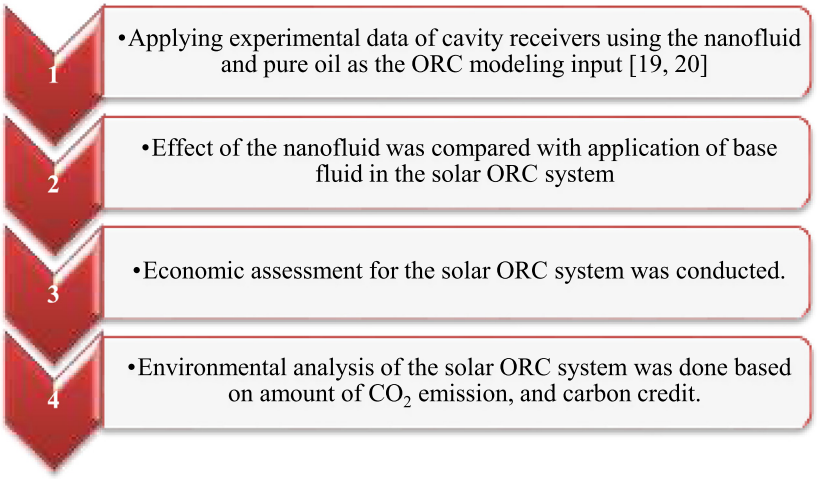

Fig. 1. A flowchart for the general methodological approach of the current study.

references of Loni et al. (2018f) and Loni et al. (2018a), were used as the input of the simulated ORC system. One of the important novelty of the current study is using experimental data as input of the ORC system for prediction of the performance of an ORC system using the nanofluid application. The main aim of the present paper is the simulation and optimization of a solar ORC system based on the examined solar setup. The main objective of this research is thermodynamically, economically, and environmentally considered performance of an ORC system using the nanofluid application and different shapes of cavity receiver that were coupled with the ORC system as the heat source. Also, the effect of nanofluid as the solar working fluid was compared with the application of base fluid in the solar ORC system. The results of this work can be used for the future design of highly efficient solar-driven ORC systems for electricity production.

2. Modeling and methodology

In this section, firstly, a general approach of the used method in this study was presented. Afterward, modeling method for simulation of the solar systems, and ORC system was explained. Finally, economical and environmental analyses of the system were presented in detail.

2.1. General approach

In this study, a solar ORC system with different types of cavity receiver and application of MWCNT/oil nanofluid was investigated in several steps as follows:

- In the first step, reported experimental data of the cavity receivers using the nanofluid and oil by the authors (Loni et al., 2018f,a), were used as the input of the ORC modeling.
- The solar ORC system efficiency was considered with various solar fluids including nanofluid and based fluid.
- Thermodynamic efficiency was evaluated for the various types of cavity receiver effects, namely cylindrical and hemispheric receivers.
- Economic assessment for the solar ORC system was conducted.
- Environmental analysis of the solar ORC system was done based on the amount of CO_2 emission, and carbon credit.

A flowchart of the general methodological approach of the current study was presented in Fig. 1.

2.2. Specification of solar system

As mentioned in the above, the experimentally measured data by the authors (Loni et al., 2018f,a), was used as the input of the ORC modeling. In other words, the thermodynamic performance of the cavity receivers as heat supply to the ORC system was investigated and optimized for further experimental ORC studies. Fig. 2a represents a view of the used focal point concentrator setup during the experimental tests. The focal point concentrator has 1.9 m diameter of the aperture, 1 m of focal distance and 1°tracking error. A schematic of the solar dish concentrator with the cylindrical and hemispherical cavity receivers is given in Fig. 3. Copper tubes with a diameter of 10 mm were used as the cavity tubes. The cavity tubes were selectively coated with Black Chrome to improve absorption. For the reduction of heat loss, the cavity receivers were isolated with mineral wool. All structural measurements of the cavity receivers were selected and constructed based on the authors' optimization studies (Loni et al., 2016a, 2017a). Fig. 2b, and c, respectively, showed a view of the cylindrical and hemispheric cavity receivers.

On the other side, nanofluid is implemented as an efficient way to improve thermal efficiency. The application of the nanofluid with the mass fraction of 0.8% and pure oil as the base fluid was examined in the cavity receivers. The authors have tested the solar dish concentrator's thermal performance with two cavity receiver shapes using MWCNT/oil nanofluid, and pure oil during a day in Refs. Loni et al. (2018f) and Loni et al. (2018a). They measured operational parameters including the working fluid temperature at cavity receiver inlet and outlet, and working fluid flow rate and environmental parameters including air temperature, wind speed and solar radiation. A view of the investigated MWCNT nanoparticles is depicted in Fig. 4. More details related to the experimental tests were reported in Refs. Loni et al. (2018f) and Loni et al. (2018a). Generally, the MWCNT/oil nanofluid was selected due to its perfect thermal properties as presented in Table 1 as well as perfect sustainability with no sedimentation during nine-month (Loni et al., 2018f). Also, Behran thermal oil has been used as the base fluid with the following thermal properties (Loni et al., 2016):

$$k_f = 0.1882 - 8.304 \times 10^{-5}\left(T_f\right) \quad \left(\frac{\mathrm{W}}{\mathrm{m\ K}}\right) \tag{1}$$

$$c_{p,f} = 0.8132 + 3.706 \times 10^{-3}\left(T_f\right) \quad \left(\frac{\mathrm{kJ}}{\mathrm{kg\ K}}\right) \tag{2}$$

$$\rho_f = 1071.76 - 0.72\left(T_f\right) \quad \left(\frac{\mathrm{kg}}{\mathrm{m}^3}\right) \tag{3}$$

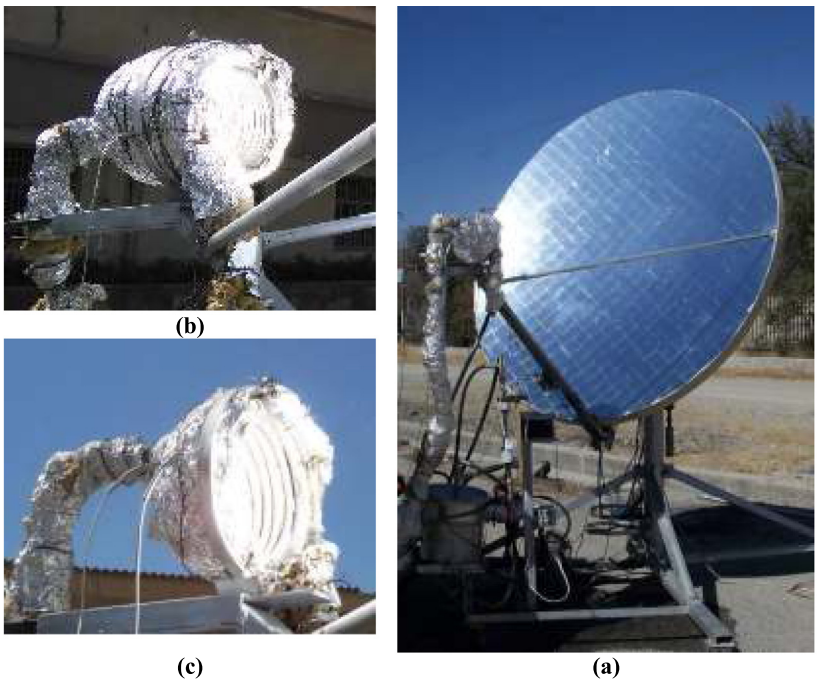

Fig. 2. Used experimental setup, (a) focal point concentrator (Loni et al., 2017a), (b) cylindrical cavity, and (c) hemispherical cavity receiver (Loni et al., 2018d).

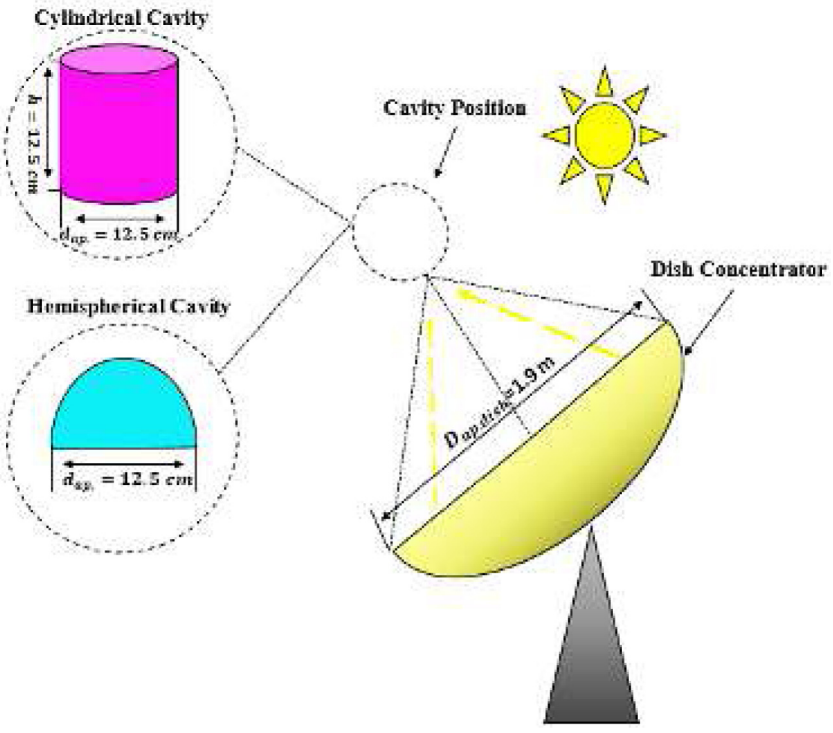

Fig. 3. A schematic of the solar dish concentrator with the cylindrical and hemispherical cavity receivers.

$$Pr = 6.73899 \times 10^{21} \left(T_f\right)^{-7.7127} \quad (4)$$

In these equations, T_f (K) is the temperature working fluid, k_f ($\frac{W}{m\ K}$) is working fluid conductivity, $c_{p,f}$ ($\frac{kJ}{kg\ K}$) is the working fluid special heat capacity, ρ_f ($\frac{kg}{m^3}$) density of the working fluid, and Pr is the working fluid Prandtl number.

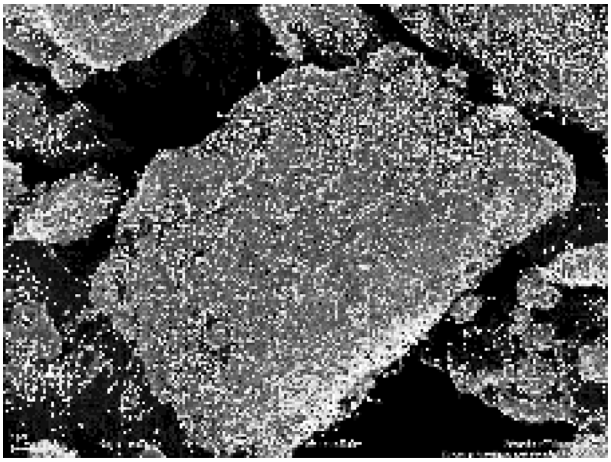

Fig. 4. A view of the investigated MWCNT nanoparticles.

Table 1
Thermal properties of the MWCNT nanoparticles.

Property	MWCNT
Thermal conductivity (W/m K)	2000
Specific heat (J/kg K)	733
Density (kg/m^3)	2100

It should be mentioned, there are chain investigations that are done by the authors on the dish concentrator. In this research, experimental results were used as heat sources of an ORC electricity generation system for cylindrical and hemispheric cavity receiver. The solar ORC system has been investigated as a new subject for study, based on energy, economic, and environmental aspects.

2.3. ORC modeling

In this research, the measured absorbed heat by the focal point concentrator with the cavity receivers as the heat source of the ORC device for power generation has been investigated. A diagram of the Solar ORC system is given in Fig. 5. The ORC system is accounted as an efficient thermodynamic cycle including an evaporator for absorbing heat, a turbine for power generation, a condenser for ORC working fluid cooling, and a pump for working fluid circulation. It should be mentioned that absorbing heat will be occurred at constant pressure, generating power will be done under isentropic condition, ejecting heat at constant pressure, and pressurizing working fluid at the isentropic condition. The ORC device was investigated in this research at 3 MPa constant evaporator pressure and 311 K condenser temperature. A view of the T-s diagram of the ORC system is presented in Fig. 6.

ORC working fluid thermodynamic properties were determined using the REFPROP.8 software (Lemmon et al., 2007). The R113 was selected as the ORC work fluid based on reported results by Ref. Shahverdi et al. (2019). The thermophysical properties of R113 are presented in Table 2. In this analysis, the absorbed heat from the solar system was supposed to be transferred to the working fluid of the ORC in the evaporator. Therefore, the flow rate of the organic fluid ($\dot{m}_{ORC}$) can be estimated as (Cengel, 2011):

$$\dot{m}_{ORC} = \frac{\dot{Q}_{evp}}{(h^*_3 - h^*_2)} \tag{5}$$

where, $\dot{Q}_{evp}$ (W) is the measured absorbed heat by the solar systems, h^*_2 (kJ/kg) and h^*_3(kJ/kg) are ORC work fluid enthalpy at the evaporator inlet and outlet.

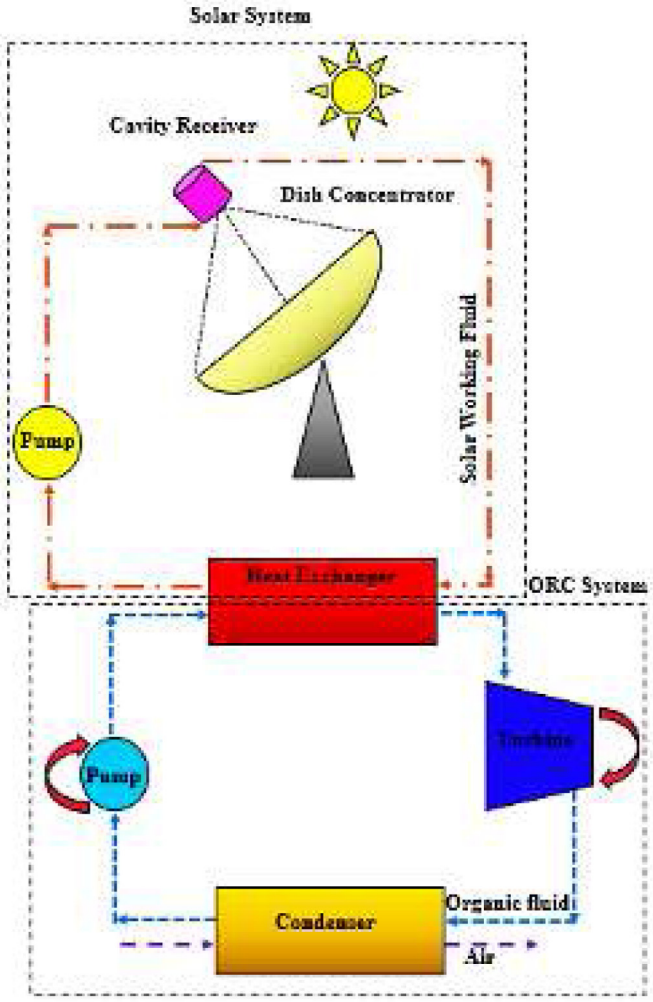

Fig. 5. A schematic of the solar ORC system.

The generated power by the turbine ($\dot{W}_T$), ejected heat by the condenser ($\dot{Q}_c$), and consumed energy by the pump ($\dot{W}_P$) can be calculated as following (Cengel, 2011):

The power generated in the turbine can be calculated by the following equation:

$$\dot{W}_T = \dot{m}_{ORC}\left(h^*_3 - h^*_4\right) \tag{6}$$

$$\dot{Q}_c = \dot{m}_{ORC}\left(h^*_4 - h^*_1\right) \tag{7}$$

$$\dot{W}_P = \dot{m}_{ORC}(h^*_2 - h^*_1) \tag{8}$$

where, h^*_4(kJ/kg), and h^*_1 (kJ/kg) are the enthalpy at the outlet of the turbine, and enthalpy at the inlet of the pump, respectively. Consequently, the net power of the ORC system ($\dot{W}_{net}$), ORC efficiency (η_{ORC}), and overall solar ORC efficiency ($\eta_{overall}$) can be estimated as follows:

$$\dot{W}_{net} = \dot{W}_T - \dot{W}_P = \dot{m}_{ORC}[\left(h^*_3 - h^*_4\right) - \left(h^*_2 - h^*_1\right)] \tag{9}$$

$$\eta_{ORC} = \frac{\dot{W}_{net}}{\dot{Q}_{evp}} \tag{10}$$

$$\eta_{overall} = \frac{\dot{W}_{net}}{I_{beam} \cdot A_{ap,dish}} \tag{11}$$

where, I_{beam} (W/m^2), and $A_{ap,dish}$ (m^2) are solar beam radiation, and the aperture area of the dish collector respectively.

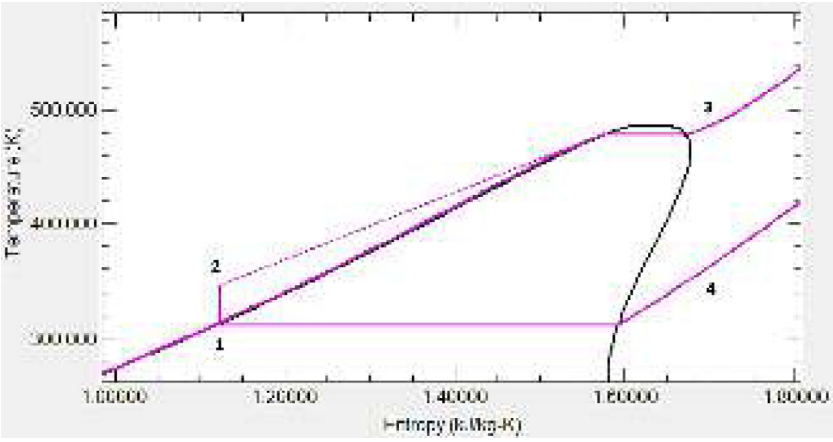

Fig. 6. The entropy–temperature diagram of the ORC system for R113.

Table 2
Thermo-physical properties of the considered working fluid.

Working fluid	Molecular mass (kg/kmol)	T_{bp} (°C)	T_{cr} (°C)	P_{cr} (MPa)
R113	187.38	47.6	214.1	3.439

The input data of the ORC modeling is presented in Tables 3, and 4, for cylindrical and hemispherical cavity receivers using the nanofluid and thermal oil respectively.

2.4. Economic analyses

This research has economically examined the established solar ORC system. Levelized Electricity Cost (LCOE) is one of the economic parameters examined; that can be described as the ORC system's investment and maintenance costs in its lifetime as (€) to the solar ORC system's generated power as kWh. The LCOE equation can be determined as follows:

$$LCOE = \frac{I_t + M_t + F_t}{E_t} \tag{12}$$

When the investment cost isI_t (€), M_t (€) is maintenance costs, F_t (€) is the fossil fuel cost presumed to be equal to zero in this analysis, with the power generated by E_t (kWh). The solar ORC device investment costs can be calculated as follows:

$$I_t = I_{t,PTC} + I_{t,ORC} \tag{13}$$

In this equation, $I_{t,PTC}$ is the solar PTC system's investment costs, which is expected to be 275 €/m^2 (Bellos and Tzivanidis, 2018a), and $I_{t,ORC}$ is the ORC system's investment cost estimated to be 3000 €/kWh (Bellos and Tzivanidis, 2018a). The following equation can be provided in relation to solar ORC system maintenance costs:

$$M_t = 0.01 \cdot N \cdot I_t \tag{14}$$

where N is the approximate solar ORC system's lifetime, which in this research was assumed to be equivalent to 25 years, and I_t is the investment cost calculated based on the previous equations of the solar ORC system. The power generated, E_t (kWh), can finally be determined in the following way:

$$E_t = N \cdot E_{t,yearly} \tag{15}$$

where $E_{t,yearly}$ (kWh) is power produced by the solar ORC system on an annual basis, and N is the approximate solar ORC system's lifetime assumed to be equivalent to 25 years in this research. Cash flow is another metric that is used for economic analysis. The annual income minus maintenance costs can be calculated as cash flow:

$$CF = \left[E_{t,yearly} \cdot C_{el}\right] - M_t \tag{16}$$

The cash flow in this equation is CF (€), while the financial value of the electricity generated is C_{el} (€/kWh) expected to be 0.2 in this case (Bellos and Tzivanidis, 2018a).

Eventually, another significant parameter for a system's economic analysis is the Simple Payback Period (SPP). The SPP is known as how long to be profitable for the system. The calculation of the SPP is as follows:

$$SPP = \frac{I_t}{CF} \tag{17}$$

2.5. Environmental aspects

The application of renewable energies is recommended due to their positive effects on reducing greenhouse gas emissions. Current research has studied the environmental effects of solar energy as a heat source and the ORC technology for the generation of electricity through waste heat from desalination systems. Amounts of CO_2 mitigated per annum can be estimated based on the following equation (Sahota and Tiwari, 2017):

$$\varphi_{CO_2} = \frac{\psi_{CO_2} \times E_{en,ann}}{10^3} \tag{18}$$

where, φ_{CO_2}(ton) is CO_2 emission per annum, ψ_{CO_2} (kgCO_2/kWh) is average CO_2 producing for power generation from coal that was assumed equal to 2.04, and $E_{en,ann}$ (kWh) is power generation by the solar or ORC systems during a year, whereas each year was assumed 2500 hr for Tehran, Iran as a case study. Also, carbon credit (Z_{CO_2}) was investigated as another important environmental parameter as followings (Sahota and Tiwari, 2017):

$$Z_{CO_2} = z_{CO_2} \times \varphi_{CO_2} \tag{19}$$

where, Z_{CO_2} ($) is carbon credit per annum, z_{CO_2} ($/ton) is carbon credit which was assumed equal to 14.5, and φ_{CO_2} (ton) is CO_2 emission per annum (Sahota and Tiwari, 2017).

3. Results and discussion

The findings of the solar ORC system using the cylindrical and hemisphere cavity receivers will be described in three subsections as below:

- Firstly, the solar ORC system will be analyzed thermally and thermodynamically.

Table 3
Measured data of the cylindrical cavity receiver using (a) MWCNT/oil nanofluid and (b) pure oil.

Time	Q_{in} (W)	I_{beam} (W/m^2)	T_{amb} (°C)	Time	Q_{in} (W)	I_{beam} (W/m^2)	T_{amb} (°C)
(a)				(b)			
10:00	975.64	629.8	27.5	9:10	1010.42	642.40	25.4
10:30	1106.00	674.6	23.1	9:30	1124.31	706.52	27.5
10:45	1324.34	738.0	23.4	10:00	1111.99	691.58	25.6
11:00	1367.36	748.4	24.0	10:30	1133.80	672.77	24.1
11:30	1372.59	750.0	25.4	11:00	1102.07	677.20	25.0
11:50	1360.35	750.0	25.0	11:30	1121.71	683.27	25.7
12:30	1328.33	734.0	23.0	12:15	1138.05	684.32	27.3
12:52	1264.35	709.7	23.0	12:30	1149.04	691.74	27.9
13:00	1266.05	706.5	22.6	13:00	1093.42	676.23	28.4
13:30	1127.62	646.3	25.2	13:30	1080.25	670.31	27.7
14:00	1075.88	623.1	25.9	14:00	1061.42	665.42	27.2
14:30	962.49	566.3	27.7	14:30	1131.38	674.79	26.7
15:00	808.45	515.5	26.5	15:00	1042.51	640.65	26.2
				15:30	840.55	525.85	27.2
				15:50	784.03	524.38	26.0

Table 4
Measured data of the hemispherical cavity receiver using (a) nanofluid, and (b) thermal oil.

Time	Q_{in} (W)	I_{beam} (W/m^2)	T_{amb} (°C)	Time	Q_{in} (W)	I_{beam} (W/m^2)	T_{amb} (°C)
(a)				(b)			
10:15	1087.71	595.05	20.6	9:30	1335.25	752.82	26.9
10:40	1252.38	625.13	21.0	10:00	1394.94	774.27	27.8
11:15	1429.46	657.23	22.1	10:30	1478.96	790.79	28.0
11:30	1455.19	667.64	23.0	11:00	1530.17	805.02	29.0
12:15	1387.78	642.23	21.6	11:15	1566.74	824.22	29.0
12:40	1372.31	640.87	21.6	11:45	1637.74	849.04	31.3
13:00	1360.18	635.42	21.0	12:30	1656.08	859.22	31.6
13:30	1346.65	632.97	20.2	13:00	1615.43	841.63	31.5
14:00	1075.44	567.82	20.5	13:30	1591.46	833.46	31.0
14:30	781.62	503.88	21.0	13:45	1542.19	810.56	31.0
15:00	533.80	432.69	20.6	14:00	1375.60	774.60	30.0
				14:30	1237.66	728.86	30.0
				15:30	987.63	656.61	28.0
				16:00	926.13	623.30	27.5

- Then, economic performance results will be recorded for the solar ORC system.
- Finally, the solar ORC system's environmental performance related to CO_2 emission and carbon credits will be presented.

3.1. Thermal and thermodynamic analyses

In this section, the suggested ORC system with two shapes of cavity receiver as heat source of the ORC system, was investigated based on thermodynamic analyses. Also, a comparison performance of both investigated solar ORC systems was presented.

3.1.1. Cylindrical cavity receiver

Fig. 7a displays a comparison of produced ORC net power with the cylindrical cavity receiver use specific solar working fluids as the ORC heat source. During this comparison study, nanofluid with 0.8% mass fraction of nanoparticles, and pure oil have been used as the solar fluid. R113 has been used as a fluid for ORC. As seen, the produced ORC net power is higher when using MWCNT/oil nanofluid.

On the other side, Fig. 7b depicts a comparison study of total efficiency with the application of nanofluid, and base fluid. The focal point concentrator using the cylindrical cavity receiver has been used as an ORC heat source. Nanofluid with nanoparticle mass fraction of 0.8% was experimentally prepared and tested as the nanofluid. As concluded from Fig. 7b, the nanofluid application has increased the overall efficiency of the Solar ORC system.

Cavity thermal efficiency and total ORC efficiency using nanofluid and pure oil have been compared in Table 5. The cylindrical cavity receiver has been tested experimentally and used as the source of ORC power. It should be mentioned that the reported data in Table 5 are for the steady-state period. As resulted, the ORC total efficiency of the solar ORC system has increased using the nanofluid. The average of the total ORC efficiency utilizing the nanofluid was calculated to be equal to 17.8%, whereas the average of the total ORC efficiency using pure oil was reported to be equal to 15.8%, in the time of steady-state during the experimental tests. Also, the average performance cavity with nanofluid has been reported to be 63.9%, and, one using pure oil was reported to be equal to 57.6%, in the steady-state period.

Table 5
Cavity thermal efficiency and total ORC efficiency using nanofluid, and pure oil with the cylindrical cavity receiver.

Solar working fluid	Pure oil		MWCNT/oil nanofluid	
Parameters	$\eta_{total,solar\ ORC}$	$\eta_{th,cavity}$	$\eta_{total,solar\ ORC}$	$\eta_{th,cavity}$
Steady-state period	0.162	0.574	0.178	0.635
	0.163	0.579	0.181	0.647
	0.165	0.587	0.182	0.648
	0.165	0.586	0.180	0.642
	0.161	0.571	0.180	0.640
	0.160	0.569	0.177	0.630
	0.158	0.563	0.178	0.634
Average	0.162	0.576	0.179	0.639

3.1.2. Hemispherical cavity receiver

Produced ORC net power using nanofluid and pure oil as the solar working fluids is reported in Fig. 8a during the experimental tests. A focal point concentrator tested using a hemisphere cavity receiver and used as a supply of heat to ORC. The

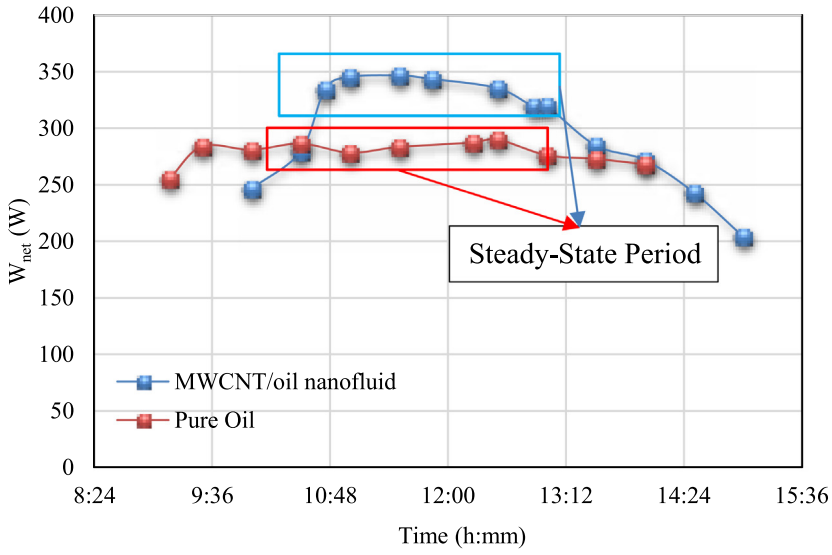

(a)

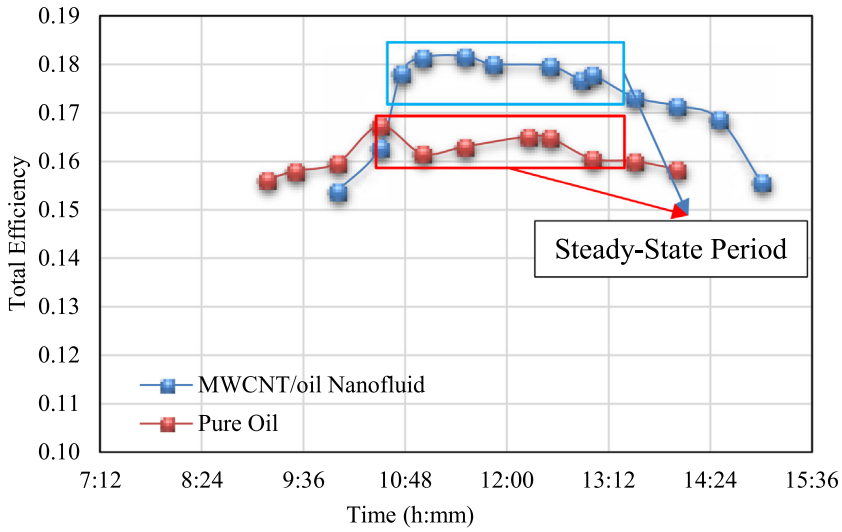

(b)

Fig. 7. Comparison of (a) ORC net power and (b) total efficiency of the cylindrical cavity receiver using nanofluid, and oil as the heat transfer fluid, with R113 as the ORC working fluid.

MWCNT/oil nanofluid was experimentally prepared and examined with nanoparticles mass fraction of 0.8%. As resulted from Fig. 8a, the generated ORC net power using the nanofluid shows lower amounts. This is because of the lower amount of incoming solar irradiation during the experimental nanofluid tests. On the other side, amounts of the ORC total efficiency using the MWCNT/oil nanofluid, and pure oil is shown in Fig. 8b during the experimental tests. As concluded from Fig. 8b, the total ORC efficiency of the Solar ORC device investigated indicates higher quantities for nanofluid use. The steady-state period of the experimental tests was displayed in Fig. 8 for the nanofluid and pure oil application. Based on Fig. 8b, the total ORC output of the Solar ORC system also has higher values in the steady-state period compared to the pure oil.

Cavity thermal efficiency and total solar ORC efficiency by the nanofluid and the pure oil during the steady-state period were compared in Table 6. Experimental data using the nanofluid with the nanoparticle mass fraction of 0.8% and pure oil were used as the heat supply for the ORC. As seen, the average amount of the total ORC efficiency with the application of the nanofluid is equal to 21.4%, while this value is calculated to be equal to 18.9% with the use of the pure oil as based-fluid. Also, the solar thermal efficiency was measured to be equal to 76.2% for the nanofluid, and average thermal efficiency is reported to be equal to 67.5% for the pure oil case. It would be concluded from Table 6, the hemispheric cavity receiver solar system thermal efficiency with nanofluid use has increased. Total solar ORC performance of the hemisphere cavity solar ORC system has been enhanced by the application of nanofluid. The use of the MWCNT/Oil nanofluid is therefore suggested as a good way to improve the solar ORC system's performance.

3.1.3. Comparison of cavity receivers

In this segment, a variation of ORC performance parameters using cavity receivers as the ORC heat sources was investigated.

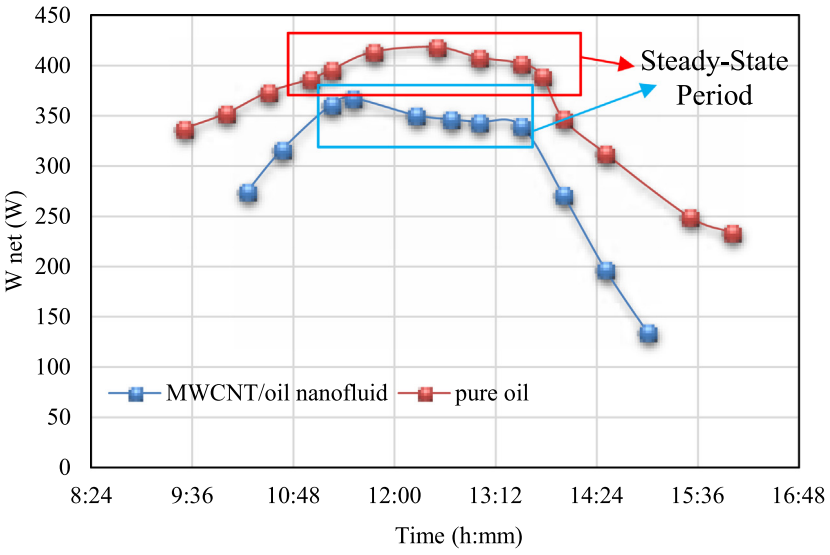

(a)

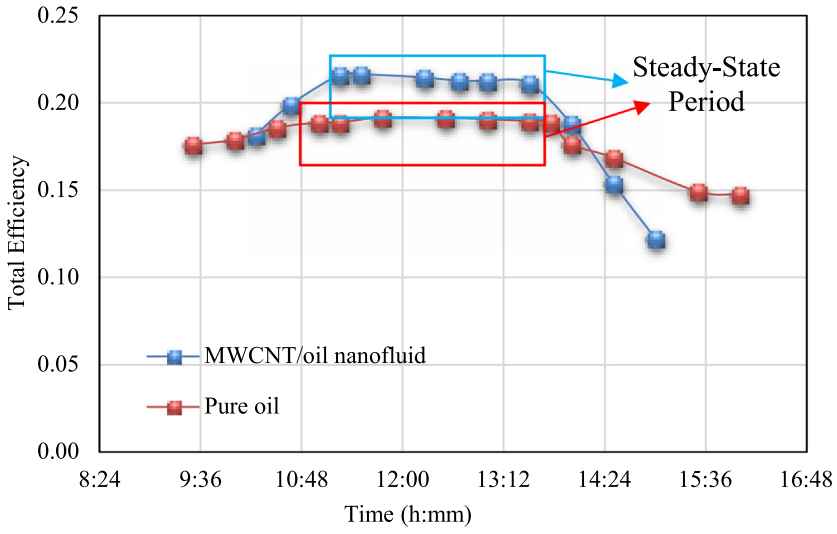

(b)

Fig. 8. Comparison of (a) ORC net power, and (b) total efficiency for hemispherical cavity as the ORC heat source and R113 as the ORC working fluid.

Table 6
Cavity thermal efficiency and total ORC efficiency using the nanofluid, and pure oil with the hemispherical cavity receiver.

Solar working fluid	Pure oil		MWCNT/oil nanofluid	
Parameters	$\eta_{total,solar\ ORC}$	$\eta_{th,cavity}$	$\eta_{total,solar\ ORC}$	$\eta_{th,cavity}$
Steady-state period	0.186	0.662	0.216	0.770
	0.189	0.673	0.216	0.771
	0.189	0.673	0.215	0.765
	0.192	0.683	0.213	0.758
	0.191	0.682	0.213	0.757
	0.191	0.679	0.211	0.753
	0.190	0.676		
	0.189	0.673		
Average	0.189	0.675	0.214	0.762

Two different cavity shapes have been studied including a cylindrical cavity and hemispheric cavity receivers. Fig. 9a displays the ORC net power variations for the cavity receivers. Note that cavity receiver data are based on experimental tests using MWCNT/oil nanofluids. The experimental data have been used as the model Solar ORC system heat source data. As seen, the ORC net power indicates higher quantities using the hemisphere cavity receiver then the cylindrical cavity receiver as the solar dish absorber. Fig. 9b further describes changes in the overall ORC efficiency for cylindrical and hemispheric cavity receiving systems as the ORC heat supply. In comparison to the cylindrical receiver as ORC thermal source, it could be determined that the overall ORC efficiency of the solar ORC system has improved with the hemisphere cavity. As a result, the hemispheric cavity receiver is suggested as a more powerful cavity compared to the cylindrical cavity for generating power from the solar ORC heat source.

Table 7 reports the variation of the ORC performance parameters and environmental parameters for the cylindrical cavity. Note that R113 is used as a fluid for the ORC system, and the nanofluid has been tested. It would be seen from Table 7, the ORC

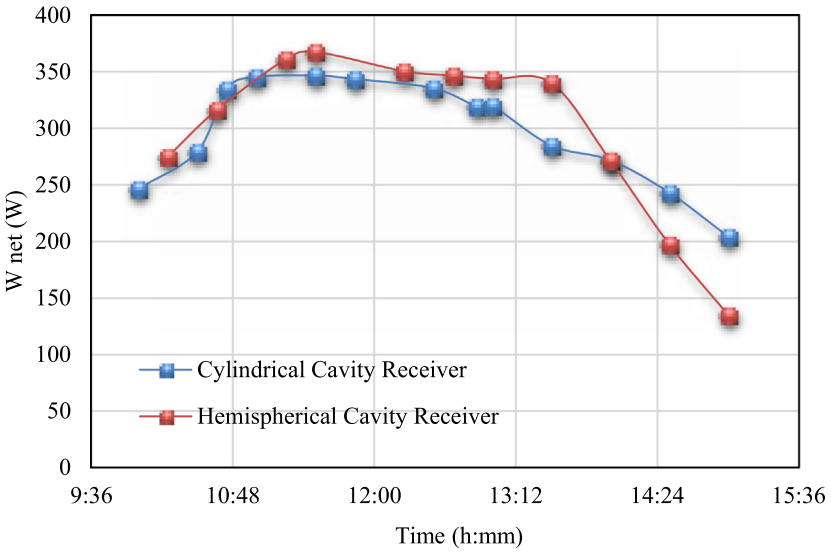

(a)

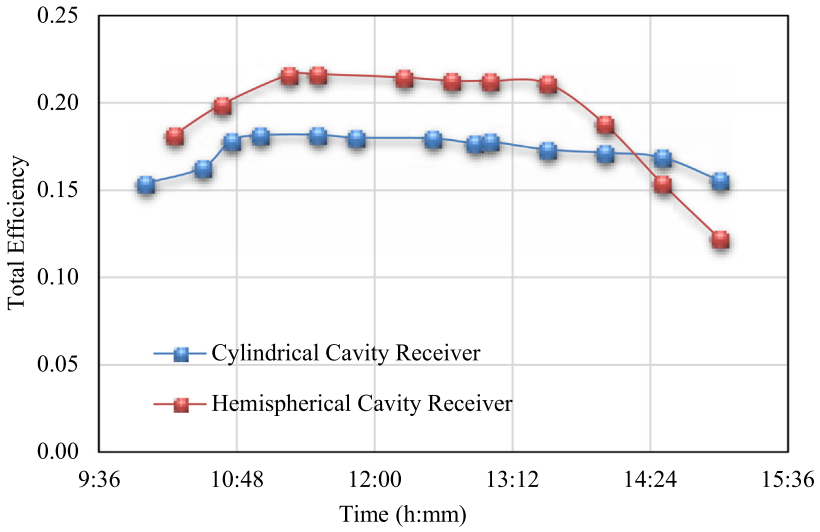

Fig. 9. Variation of (a) ORC net power, and (b) total efficiency for cylindrical and hemispherical cavity receivers using R113 as the ORC working fluid, and the nanofluid as the solar working fluid.

net power ($\dot{W}_{net}$), generated turbine power ($\dot{W}_{turbine}$), consumed pump power ($\dot{W}_{pump}$), ejected heat from the condenser ($\dot{Q}_{cond}$), and ORC mass flow rate ($\dot{m}_{ORC}$) have a direct relation with heat gain from the cavity ($\dot{Q}_{\text{in}}$). The cavity heat gain shows a direct relationship with the solar irradiation (I_{beam}) as reported during the experimental test. The same findings were recorded as the ORC heat source using the MWCNT/oil nanofluid in Table 8 for the hemispheric cavity receiver.

3.2. Economic analyses

This segment discusses the economic analyses of the solar ORC system. Variation of Levelized Cost of Electricity (LCOE), Cash Flow (CF), and Simple Payback Period (SPP) of the solar system are reported in Table 9 during the steady-state conditions. Two different types of cavity receivers have been studied including a nano-fluid cylindrical and hemispherical receiver. As understood from Table 9, the average amount of the LCOE during the steady-state condition was found to be equivalent to 0.077 €/kWh and 0.076 €/kWh for the cylindrical and hemispherical cavity receiver as an ORC heat supply, respectively. As seen, the ORC system with the hemispherical cavity receiver resulted in a lower cost for the generated power. Also, in Table 9, average amounts of the CF during the steady-state condition were estimated equal to 16589.76 €/year, and 17414.92 €/year for the cylindrical and hemispherical cavity receiver as the ORC heat supply, respectively.

As a result, the hemispheric cavity receiver ORC system generated a higher amount of electricity during a year. Finally, as resulted in Table 9, average amounts of the SPP during the steady-state condition were calculated as 9.541 years, and 9.374 years for the cylindrical and hemispherical cavity receiver as the ORC heat supply, respectively. Consequently, the hemispheric cavity receiver ORC system can be suggested as a more economical system for power generation.

3.3. Environmental analyses

This segment has addressed environmental analyses of the solar ORC system. Table 10 reports the variation of CO_2 emission (φ_{CO_2}), and CO_2 credits (Z_{CO_2}), for the solar dish collector with the

Table 7
Variation of the ORC performance for cylindrical cavity receiver using R113 as the ORC working fluid and the nanofluid.

Time	T_{amb} (°C)	I_{beam} (W/m^2)	V_{wind} (m/s)	$\dot{Q}_{in}$ (W)	$\dot{m}_{ORC}$ (gr/s)	$\dot{Q}_{cond}$ (W)	$\dot{W}_{pump}$ (W)	$\dot{W}_{turbine}$ (W)	$\dot{W}_{net}$ (W)
10:00	27.5	629.80	1.1	975.64	4.22	729.22	0.0081	246.43	246.42
10:30	23.1	674.60	1.7	1106.00	4.78	826.66	0.0091	279.35	279.35
10:45	23.4	738.00	2.5	1324.34	5.72	989.85	0.0109	334.50	334.49
11:00	24.0	748.40	1.3	1367.36	5.91	1022.00	0.0113	345.37	345.36
11:30	25.4	750.00	1.7	1372.59	5.93	1025.91	0.0113	346.69	346.68
11:50	25.0	750.00	1.7	1360.35	5.88	1016.76	0.0112	343.60	343.59
12:30	23.0	734.00	0.0	1328.33	5.74	992.83	0.0110	335.51	335.50
12:52	23.0	709.70	0.3	1264.35	5.46	945.01	0.0104	319.35	319.34
13:00	22.6	706.50	0.2	1266.05	5.47	946.28	0.0105	319.78	319.77
13:30	25.2	646.30	1.4	1127.62	4.87	842.82	0.0093	284.82	284.81
14:00	25.9	623.10	2.4	1075.88	4.65	804.14	0.0089	271.75	271.74
14:30	27.7	566.30	1.3	962.49	4.16	719.39	0.0079	243.11	243.10
15:00	26.5	515.50	2.2	808.45	3.49	604.26	0.0067	204.20	204.19

Table 8
Variation of the ORC performance for hemispherical cavity receiver using R113 as the ORC working fluid and the nanofluid.

Time	T_{amb} (°C)	I_{beam} (W/m^2)	V_{wind} (m/s)	Q_{in} (W)	m_{ORC} (gr/s)	Q_{cond} (W)	W_{pump} (W)	$W_{turbine}$ (W)	W_{net} (W)
10:15	20.6	595.05	1.0	1087.71	4.70	812.99	0.0090	274.74	274.73
10:40	21.0	625.13	0.2	1252.38	5.41	936.07	0.0103	316.33	316.32
11:15	22.1	657.23	0.2	1429.46	6.18	1068.42	0.0118	361.05	361.04
11:30	23.0	667.64	1.3	1455.19	6.29	1087.65	0.0120	367.55	367.54
12:15	21.6	642.23	2.5	1387.78	6.00	1037.27	0.0115	350.53	350.52
12:40	21.6	640.87	0.0	1372.31	5.93	1025.70	0.0113	346.62	346.61
13:00	21.0	635.42	0.0	1360.18	5.88	1016.63	0.0112	343.55	343.54
13:30	20.2	632.97	0.6	1346.65	5.82	1006.53	0.0111	340.14	340.13
14:00	20.5	567.82	1.1	1075.44	4.65	803.82	0.0089	271.64	271.63
14:30	21.0	503.88	0.9	781.62	3.38	584.20	0.0065	197.42	197.42
15:00	20.6	432.69	1.6	533.80	2.31	398.97	0.0044	134.83	134.82

Table 9
Variation of Levelized Cost of Electricity (LCOE), Cash Flow (CF), and Simple Payback Period (SPP) of the cylindrical and hemispherical cavity during the steady-state conditions.

Cylindrical cavity receiver			
Time (hh:mm)	LCOE (€/kWh)	CF (€/year)	SPP (years)
10:45	0.078	16 566.45	9.542
11:00	0.077	17 106.45	9.432
11:30	0.077	17 172.16	9.419
11:50	0.077	17 018.49	9.449
12:30	0.077	16 616.56	9.532
12:52	0.079	15 813.43	9.709
13:00	0.079	15 834.81	9.704
Average	0.077	16 589.76	9.541
Hemispherical cavity receiver			
Time (hh:mm)	LCOE (€/kWh)	CF (€/year)	SPP (years)
11:15	0.075	17 886.04	9.284
11:30	0.075	18 209.01	9.226
12:15	0.076	17 362.88	9.381
12:40	0.077	17 168.67	9.419
13:00	0.077	17 016.32	9.450
13:30	0.077	16 846.58	9.484
Average	0.076	17 414.92	9.374

Table 10
Variation of CO_2 emission (φ_{CO_2}), and CO_2 credits (Z_{CO_2}), for the solar dish collector with the cylindrical and hemispherical cavity, and the ORC system during the steady-state conditions.

Cylindrical cavity receiver				
Time (hh:mm)	Dish collector		ORC system	
	φ_{CO_2} (ton/year)	Z_{CO_2} ($)	φ_{CO_2} (ton/year)	Z_{CO_2} ($)
10:45	675.41	9793.47	448.92	6509.36
11:00	697.35	10 111.59	463.50	6720.80
11:30	700.02	10 150.31	465.28	6746.54
11:50	693.78	10 059.77	461.13	6686.36
12:30	677.45	9823.00	450.27	6528.99
12:52	644.82	9349.86	428.59	6214.51
13:00	645.69	9362.46	429.16	6222.88
Average	676.36	9807.21	449.55	6518.49
Hemispherical cavity receiver				
Time (hh:mm)	Dish collector		ORC system	
	φ_{CO_2} (ton/year)	Z_{CO_2} ($)	φ_{CO_2} (ton/year)	Z_{CO_2} ($)
11:15	729.02	10 570.86	484.56	7026.06
11:30	742.15	10 761.12	493.28	7152.52
12:15	707.77	10 262.66	470.43	6821.22
12:40	699.88	10 148.25	465.18	6745.17
13:00	693.69	10 058.50	461.07	6685.51
13:30	686.79	9958.50	456.49	6619.05
Average	709.88	10 293.31	471.83	6841.59

cylindrical and hemispherical cavity, and the ORC system during the steady-state conditions. The nanofluid and R113 have been used as the solar and ORC fluid.

The average amount of the CO_2 emission for the dish concentrator, and the ORC system during the steady-state condition were calculated equal to 676.36 ton/year and 449.55 ton/year for the cylindrical cavity receiver as the source of heat for the ORC system, respectively. Also, average amounts of the CO_2 emission for the dish concentrator, and the ORC system during the steady-state condition were estimated as 709.88 ton/year and 471.83 ton/year for the hemispheric cavity receiver as an ORC heat supply, respectively. Some similar results were achieved for the amount of CO_2 credit. Consequently, it could be concluded that the solar ORC device with the hemisphere cavity receiver as the heat source for ORC had resulted in more positive environmental influence related to the cylindrical one.

4. Conclusions

A solar ORC system using cavity receivers was considered in this work. A focal point concentrator was studied as an ORC heat

source with two types of receiver, one cylindrical and the other hemisphere. For solar working fluid, MWCNT/oil nanofluid and pure oil were used. R113 was considered a working fluid for ORC. The ORC modeling was developed based on the previous experimental tests of the authors. The main achieved results can be summarized as the following:

- The solar ORC system has the highest amount of ORC performance parameters using MWCNT/oil nanofluid. The use of nanofluid in a hemispheric receiver is therefore proposed as an efficient way to improve solar ORC system performance.
- Average of the total ORC efficiency using the nanofluid was calculated to be equal to 17.8%, whereas the average of the total ORC efficiency using pure oil was reported to be equal to 15.8%, for the cylindrical cavity receiver as the source of heat to the ORC during experimental testing during the steady-state period.
- The average amount of total ORC efficiency with nanofluid use was equal to 21.4%, while this value was calculated to be equal to 18.9% with the pure oil used by the hemispheric cavity receiver as a heat supply to the ORC.
- The financial analysis proved that the LCOE is 0.076 €/kWh with the hemispherical cavity and 0.077 €/kWh with the cylindrical cavity. The SPP Is found 9.374 years with the hemispherical cavity and 9.541 years with the cylindrical cavity. So, the financial analysis indicates that the hemispherical cavity is a better choice but both choices are viable.
- It is also found that the use of the hemispherical receiver leads to a 5% lower CO_2 avoidance compared to the cylindrical receiver.
- Finally, it was found that the ORC system with the hemispherical cavity receiver is the best choice for using it as the heat source in an ORC. All the studied, energetic, financial and environmental indicate this cavity as the proper one.

Declaration of competing interest

The authors declare that they have no known competing financial interests or personal relationships that could have appeared to influence the work reported in this paper.

CRediT authorship contribution statement

Alireza Refiei: Data curation, Writing - original draft. **Reyhaneh Loni:** Conceptualization, Methodology, Software, Validation. **G. Najafi:** Visualization, Investigation. **A.Z. Sahin:** Supervision. **Evangelos Bellos:** Writing - review & editing.

Acknowledgments

Dr. Najafi and Dr. Loni would like to thank the Tarbiat Modares University, Iran for the support under grant number of IG/39705 for the Renewable Energies of Modares Research Group. The fourth author (A.Z. Sahin) would like to acknowledge the support provided by the Deanship of Scientific Research at King Fahd University of Petroleum & Minerals (KFUPM), Dhahran, Saudi Arabia for this work under Research Grant RG171001 and by the King Abdullah City for Atomic and Renewable Energy (K.A.CARE), Saudi Arabia through Research Fellowship Program, project number KACARE182-RFP-03.

References

Alarifi, I.M., Alkouh, A.B., Ali, V., Nguyen, H.M., Asadi, A., 2019a. On the rheological properties of MWCNT-TiO2/oil hybrid nanofluid: An experimental investigation on the effects of shear rate, temperature, and solid concentration of nanoparticles. Powder Technol. 355, 157–162.

Alarifi, I.M., Nguyen, H.M., Naderi Bakhtiyari, A., Asadi, A., 2019b. Feasibility of ANFIS-PSO and ANFIS-GA models in predicting thermophysical properties of Al2O3-MWCNT/oil hybrid nanofluid. Materials 12, 3628.

Allouhi, A., Amine, M.B., Saidur, R., Kousksou, T., Jamil, A., 2018. Energy and exergy analyses of a parabolic trough collector operated with nanofluids for medium and high temperature applications. Energy Convers. Manage. 155, 201–217.

Asadi, A., 2018. A guideline towards easing the decision-making process in selecting an effective nanofluid as a heat transfer fluid. Energy Convers. Manage. 175, 1–10.

Asadi, A., Aberoumand, S., Moradikazerouni, A., Pourfattah, F., Zyła, G., Estellé, P., Mahian, O., Wongwises, S., Nguyen, H.M., Arabkoohsar, A., 2019a. Recent advances in preparation methods and thermophysical properties of oil-based nanofluids: A state-of-the-art review. Powder Technol..

Asadi, A., Alarifi, I.M., Ali, V., Nguyen, H.M., 2019b. An experimental investigation on the effects of ultrasonication time on stability and thermal conductivity of MWCNT-water nanofluid: Finding the optimum ultrasonication time. Ultrason. Sonochem. 58, 104639.

Asadi, A., Alarifi, I.M., Nguyen, H.M., Moayedi, H., 2020. Feasibility of least-square support vector machine in predicting the effects of shear rate on the rheological properties and pumping power of MWCNT–MgO/oil hybrid nanofluid based on experimental data. J. Therm. Anal. Calorim. 1–16.

Asadi, M., Asadi, A., Aberoumand, S., 2018. An experimental and theoretical investigation on the effects of adding hybrid nanoparticles on heat transfer efficiency and pumping power of an oil-based nanofluid as a coolant fluid. Int. J. Refrig. 89, 83–92.

Asadi, A., Pourfattah, F., 2019. Heat transfer performance of two oil-based nanofluids containing ZnO and MgO nanoparticles; a comparative experimental investigation. Powder Technol. 343, 296–308.

Asadi, A., Pourfattah, F., Szilágyi, I.M., Afrand, M., Zyla, G., Ahn, H.S., Wongwises, S., Nguyen, H.M., Arabkoohsar, A., Mahian, O., 2019c. Effect of sonication characteristics on stability, thermophysical properties, and heat transfer of nanofluids: A comprehensive review. Ultrason. Sonochem. 104701.

Bellos, E., Tzivanidis, C., 2018a. Assessment of linear solar concentrating technologies for Greek climate. Energy Convers. Manage. 171, 1502–1513.

Bellos, E., Tzivanidis, C., 2018b. Investigation of a hybrid ORC driven by waste heat and solar energy. Energy Convers. Manage. 156, 427–439.

Cengel, Y.A., 2011. ThermodynamicsAn Engineering Approach 5th Edition By Yunus a Cengel: ThermodynamicsAn Engineering Approach, Digital Designs.

Duangthongsuk, W., Wongwises, S., 2010. Comparison of the effects of measured and computed thermophysical properties of nanofluids on heat transfer performance. Exp. Therm Fluid Sci. 34, 616–624.

El-Emam, R.S., Dincer, I., 2017. Assessment and evolutionary based multi-objective optimization of a novel renewable-based polygeneration energy system. J. Energy Resour. Technol. 139, 012003.

Fergani, Z., Morosuk, T., Touil, D., 2019. Performances optimization and comparaison of two organic rankine cycles for cogeneration in the ciment plant. J. Energy Resour. Technol. 1–27.

Hussain, M.I., Mokheimer, E.M., Ahmed, S., 2017. Optimal design of a solar collector for required flux distribution on a tubular receiver. J. Energy Resour. Technol. 139, 012006.

Khakrah, H., Shamloo, A., Hannani, S.K., 2018. Exergy analysis of parabolic trough solar collectors using Al2O3/synthetic oil nanofluid. Sol. Energy 173, 1236–1247.

Lemmon, E., Huber, M., McLinden, M., 2007. Reference fluid thermodynamic and transport properties–REFPROP version 8.0. In: NIST Standard Reference Database, Vol. 23.

Loni, R., Asli-Ardeh, E.A., Ghobadian, B., Ahmadi, M., Bellos, E., 2018a. GMDH modeling and experimental investigation of thermal performance enhancement of hemispherical cavity receiver using MWCNT/oil nanofluid. Sol. Energy 171, 790–803.

Loni, R., Asli-Ardeh, E.A., Ghobadian, B., Bellos, E., Le Roux, W., 2018b. Numerical investigation of a solar dish concentrator with different cavity receivers and working fluids. J. Cleaner Prod..

Loni, R., Asli-Ardeh, E.A., Ghobadian, B., Kasaeian, A., Bellos, E., 2018c. Energy and exergy investigation of alumina/oil and silica/oil nanofluids in hemispherical cavity receiver: Experimental study. Energy 164, 275–287.

Loni, R., Asli-Ardeh, E.A., Ghobadian, B., Kasaeian, A., Bellos, E., 2018d. Experimental energy and exergy investigation of alumina/oil and silica/oil nanofluids in hemispherical cavity receiver. Energy.

Loni, R., Asli-Ardeh, E.A., Ghobadian, B., Kasaeian, A., Bellos, E., 2018e. Thermal performance comparison between Al 2 O 3/oil and SiO 2/oil nanofluids in cylindrical cavity receiver based on experimental study. Renew. Energy.

Loni, R., Asli-Ardeh, E.A., Ghobadian, B., Kasaeian, A., Gorjian, S., 2017a. Numerical and experimental investigation of wind effect on a hemispherical cavity receiver. Appl. Therm. Eng. 126, 179–193.

Loni, R., Asli-Ardeh, E.A., Ghobadian, B., Najafi, G., Bellos, E., 2019. Effects of size and volume fraction of alumina nanoparticles on the performance of a solar organic Rankine cycle. Energy Convers. Manage. 182, 398–411.

Loni, E.A.A.-A.R., Ghobadian, B., Kasaeian, A., 2018f. Experimental study of carbon nano tube/oil nanofluid in dish concentrator using a cylindrical cavity receiver: Outdoor tests. Energy Convers. Manage. 165, 593–601.

Loni, R., Kasaeian, A., Asli-Ardeh, E.A., Ghobadian, B., 2016a. Optimizing the efficiency of a solar receiver with tubular cylindrical cavity for a solar-powered organic Rankine cycle. Energy 112, 1259–1272.

Loni, R., Kasaeian, A., Asli-Ardeh, E.A., Ghobadian, B., Le Roux, W., 2016. Performance study of a solar-assisted organic Rankine cycle using a dish-mounted rectangular-cavity tubular solar receiver. Appl. Therm. Eng. 108, 1298–1309.

Loni, R., Kasaeian, A., Mahian, O., Sahin, A., 2016c. Thermodynamic analysis of an organic rankine cycle using a tubular solar cavity receiver. Energy Convers. Manage. 127, 494–503.

Loni, R., Kasaeian, A., Mahian, O., Sahin, A.Z., Wongwises, S., 2017b. Exergy analysis of a solar organic rankine cycle with square prismatic cavity receiver. Int. J. Exergy 22, 103–124.

Malali, P.D., Chaturvedi, S.K., Abdel-Salam, T., 2017. Performance optimization of a regenerative Brayton heat engine coupled with a parabolic dish solar collector. Energy Convers. Manage. 143, 85–95.

Pavlovic, S., Bellos, E., Loni, R., 2017. Exergetic investigation of a solar dish collector with smooth and corrugated spiral absorber operating with various nanofluids. J. Cleaner Prod..

Pavlovic, S., Loni, R., Bellos, E., Vasiljević, D., Najafi, G., Kasaeian, A., 2018. Comparative study of spiral and conical cavity receivers for a solar dish collector. Energy Convers. Manage. 178, 111–122.

Qin, J., Hu, E., Nathan, G.J., Chen, L., 2017. Concentrating or non-concentrating solar collectors for solar Aided Power Generation? Energy Convers. Manage. 152, 281–290.

Sadeghi, G., Safarzadeh, H., Ameri, M., 2019. Experimental and numerical investigations on performance of evacuated tube solar collectors with parabolic concentrator, applying synthesized Cu2O/distilled water nanofluid. Energy Sustain. Dev. 48, 88–106.

Sahota, L., Tiwari, G., 2017. Exergoeconomic and enviroeconomic analyses of hybrid double slope solar still loaded with nanofluids. Energy Convers. Manage. 148, 413–430.

Sarkar, J., 2018. A novel pinch point design methodology based energy and economic analyses of organic Rankine cycle. J. Energy Resour. Technol. 140, 052004.

Shahverdi, K., Loni, R., Ghobadian, B., Monem, M., Gohari, S., Marofi, S., Najafi, G., 2019. Energy harvesting using solar ORC system and archimedes screw turbine (AST) combination with different refrigerant working fluids. Energy Convers. Manage. 187, 205–220.

Srinivas, T., Reddy, B., 2014. Thermal optimization of a solar thermal cooling cogeneration plant at low temperature heat recovery. J. Energy Resour. Technol. 136, 021204.

Subramani, J., Nagarajan, P., Mahian, O., Sathyamurthy, R., 2018. Efficiency and heat transfer improvements in a parabolic trough solar collector using TiO 2 nanofluids under turbulent flow regime. Renew. Energy 119, 19–31.

Wong, K.V., Bachelier, B., 2014. Carbon nanotubes used for renewable energy applications and environmental protection/remediation: a review. J. Energy Resour. Technol. 136, 021601.